ARTICLE INFO
Received : December. 07, 2021
Revised : January. 04, 2022
Accepted : May. 05, 2022
CT&F - Ciencia, Tecnologia y Futuro Vol 12, Num 1 June 2022. pages 95 - 106
DOI : https://doi.org/10.29047/01225383.402

ctyf@ecopetrol.com.co

SIMULATION TOOL FOR THE ANALYSIS OF IN-SITU COMBUSTION EXPERIMENTS THAT CONSIDERS COMPLEX KINETIC SCHEMES AND DETAILED MASS TRANSFER-THEORETICAL ANALYSIS OF THE GAS PHASE CO OXIDATION REACTION

HERRAMIENTA DE SIMULACIÓN PARA EL ANÁLISIS DE EXPERIMENTOS DE COMBUSTIÓN IN-SITU QUE PERMITE EL ANÁLISIS DE SISTEMAS DE REACCIÓN COMPLEJOS Y TRANSFERENCIA DE MASA - ANÁLISIS TEÓRICO DE LA REACCIÓN DE OXIDACIÓN DE CO EN LA FASE GASEOSA

Juan Felipe Hincapié[1], Sebastian López[1], Alejandro Molina[1].*

ABSTRACT

A simulation tool was designed for analyzing various experimental setups that include the ability to model detailed chemical reaction schemes for in-situ combustion (ISC) analysis. The simulation tool was illustrated with a theoretical example to the extent of CO oxidation in a gaseous phase takes place during ISC. The models in the simulation tool are based on fundamental conservation laws, physical correlations for porous media properties, and property databases available in literature. Emphasis is made on the analysis of chemical reactions in the gas phase, a characteristic that may be useful when temperatures are above 700°C and oxygen, unburned hydrocarbons, and CO coexist. The three modules of the simulation tool: (i) Kinetic cell, (ii) One-dimensional reactor, and (iii) Combustion tube, can be used to represent in detail the processes taking place in the typical laboratory-scale equipment used to characterize ISC. Tools for the analysis of transport phenomena and multiphase reactions, present in all three models, can support the process of finding chemical kinetic parameters for an easier calculation of device-independent kinetic constants. Four applications have the simulator scope: (i) Analysis of reactions in the gas phase, (ii) Axial gradients in a kinetic cell, (iii) Pressure build-up in a combustion tube, and (iv) Ignition in a combustion tube. These examples highlight the importance that homogeneous reactions may have in these systems and the existence, under certain conditions, of concentration gradients that are normally neglected, and can affect the interpretation of ISC experiments.

RESUMEN

Se desarrolló una herramienta de simulación, diseñada para el análisis de diferentes montajes experimentales que incluye la capacidad de modelar esquemas detallados de reacciones químicas para el análisis de la combustión in-situ (CIS). La herramienta de simulación se ilustró con un ejemplo teórico de la medida en que se produce la oxidación de CO en fase gaseosa durante ISC. Los modelos en el simulador están basados en las leyes fundamentales de conservación, correlaciones físicas para propiedades de medios porosos y bases de datos de propiedades disponibles en literatura libre. Se hace énfasis en el análisis de reacciones químicas en la fase gaseosa, una característica que puede ser útil en casos donde la temperatura exceda los 700°C y, además; el oxígeno, hidrocarburos sin quemar y CO coexistan. Los tres módulos del simulador: (i) Celda cinética, (ii) Reactor unidimensional (iii) Tubo de combustión, pueden ser usados para representar en detalle los procesos que toman lugar en los equipos típicos a escala de laboratorio, usados para caracterizas CIS. Herramientas para el análisis de los fenómenos de transporte y reacciones multifásicas, presentes en los tres modelos, pueden soportar el proceso de encontrar parámetros de cinética química, facilitando el cálculo de parámetros de cinética química independientes del equipo. Cuatro aplicaciones demuestran el alcance del simulador: (i) Análisis de reacciones en fase gaseosa, (ii) Gradientes axiales en una celda cinética, (iii) El desarrollo de presión en un tubo de combustión, y (iv) Ignición en un tubo de combustión. Los ejemplos destacan particularmente la importancia que tienen las reacciones homogéneas y la existencia, bajo ciertas condiciones, de gradientes de concentración que normalmente se desprecian pero pueden afectar la interpretación de experimentos en CIS

KEYWORDS / PALABRAS CLAVE

In situ combustion | Reactive porous media | Enhanced oil recovery | Heavy oil | Multiphase flow | Simulation Tool
Combustión in-situ | Medio poroso reactivo | Recobro de crudo mejorado | Crudo pesado | Flujo multifásico | Simulador.

AFFILIATION

[1] *Universidad Nacional de Colombia, Medellín, Colombia*
**email:amolinao@unal.edu.co*

1. INTRODUCTION

In-situ combustion (ISC) is a thermal oil recovery technique where an oxidizing gas (air or air enriched with oxygen) is injected into oil reservoirs to generate heat by burning a fraction of the crude oil, forming a combustion front [1–3]. ISC seems particularly suitable for heavy oils, as oil viscosity significantly decreases as temperature increases. Furthermore, during ISC, oil production is driven by flue gases and increased pressure caused by chemical reactions [4]. An advantage of ISC over other thermal recovery methods is that most of the energy required to displace the oil is generated in the reservoir from the heat released by combustion reactions [5], thus heat losses are quite small along the wellbore. This is particularly important in very deep reservoirs, as mentioned by Rodriguez [6] and Sarathi [7].

Combustion of crude oil in porous media is a complex process not fully understood. This complexity is, to some extent, derived from difficulties associated to transferring the understanding of phenomena such as chemical reaction models, mass transfer, heterogeneity of rock formation, geomechanical issues, phase equilibrium, and heat losses from the laboratory to the field [8–11]. Understanding the behavior of chemical reactions is most relevant given that the combustion of crude oil determines the released heat, the extent of coke formation, and the composition and amount of produced gas.

Combustion tubes and kinetic cells are the experimental setups most widely used to characterize ISC. The purpose of the combustion tube is to emulate, at laboratory scale, the combustion front by considering the coupled phenomena of fluid dynamics and chemical reactions. The kinetic cell is mostly used to solely study the reactions that take place in the ISC process [12]. Kinetic cells are typically modeled as a perfectly mixed semi-batch reactor where the stationary mixture of oil and rock reacts with air that flows through the reactor [13–16]. However, previous studies report heterogeneities that cause variation in the reaction velocities throughout the cell volume [17–20]. Decoupling chemical reactions and mass transfer in kinetic cells may be important to improve the predictability obtained with ISC models. Combustion tubes are usually modeled as a one-dimensional reactor [4,21]. While the chemistry and transport processes taking place in kinetic cells and combustion tubes are the same, typically their models have not been integrated; this delays the formulation of general models while favoring experimental-specific approaches. The use of comprehensive modeling simulation tools that apply the same chemical and transport sub-models to the solution of different experimental setups seems, therefore, of interest to the ISC community.

A simulation tool is a compilation of mathematical models, thermodynamic and transport databases, and solution algorithms that predict the behavior of a particular process. An archetype example of a simulation tool is CHEMKIN [22], originally developed for the generation of kinetic expressions from experimental data. CHEMKIN's novel idea was to implement modules for different reactor setups that could operate with the same kinetic expressions. This allowed researchers to improve kinetic mechanisms as they could be easily tested in multiple experiments. A similar simulation tool for the analysis of experimental data is CANTERA [23], which solves problems where chemical kinetics, thermodynamics, and transport processes are important. However, in these two simulation tools, there are no modules particularly designed for the analysis of the combustion of crude oil in porous media.

In petroleum engineering, the application of physical modelling tools for the analysis of experimental setups normally involve traditional reservoir software such as STARS [24], ECLIPSE [25], MRST [26], and others. These computer packages are comprehensive tools that enable the simulation of thermal effects, phase equilibrium, flow in porous media, chemical reactions, and geomechanical effects [27,28]. In fact, they can model ISC. However, the traditional reservoir physical modeling tools were developed to correctly predict oil extraction, and not for kinetic analysis. Their application to the small-scale experiments used in the laboratory to characterize ISC is difficult, as the complexity of reservoir simulation can obscure the kinetic analysis sought in the experiments [29]. Furthermore, in some cases it is desirable to use detailed mass transfer modelling, such as gas-phase molecular diffusion.

Computational Fluid Dynamics (CFD) packages, such as ANSYS [30] and OPEN-FOAM [31], can be also considered comprehensive simulation tools, but their application to combustion and oil flow in porous media is complex as they lack the features demanded by reservoir modeling and imply a high computation cost. The referred literature did not present evidence of simulation tools developed in particular for experimental ISC that can handle complex kinetic schemes and detailed molecular diffusion such as the one described in this study. This paper describes and validates such a simulation tool.

2. MODEL FORMULATION

The simulation tool was designed with subroutines coded in modular blocks that use common calculations among the different reactor models. Figure A.1 presents the flowchart of the simulation tool. Blocks include input data such as reactor conditions and species transport, and thermodynamic properties. Output subroutines present the user with results such as species concentration, temperature, pressure, and performance of the numerical solver. Post-processing of the results provides additional information that is particularly interesting for ISC analysis such as saturation (defined as the volume of fluid per unit of porous volume) and species reaction rates.

Cantera [23], an object-oriented, free-source software, was coupled with the simulation tool through Matlab, using Windows architecture. Cantera was used to interpret complex homogeneous reaction mechanisms, and thermodynamic and transport databases into code language that could be used in the mole and energy balances described below. Cantera provides estimates for all the thermodynamic and transport data used in the simulation toolbox. The gas properties and gas-phase kinetic parameters were taken from GRI-Mech 3.0 which contains 325 reactions and 53 species designed to model natural gas combustion [32]. The Simulation toolbox can easily include other more sophisticated reaction

mechanisms that are available in the literature (e.g. [33]), and that can account for the gas-phase oxidation of more complex substances such as diesel and gasoline.

Three modules were developed seeking to represent experimental setups to study the ISC process. The kinetic cell module involves a model which main purpose is the study of oil reactivity. The one-dimensional reactor is used to represent the axial dispersion of gas in a kinetic cell. In this module, only the gas phase flows through the cell, a reasonable assumption in an ramped temperature oxidation (RTO) experiment where all the oil is consumed in the cell. Finally, the combustion tube module shows a more realistic representation of the pressure and temperature profiles in an ISC characterization experiment. This module allows for oil, gas, and water flow. The three modules are explained in further detail in the sections below.

KINETIC CELL

Figure 1 shows the typical experimental setup of a kinetic cell, i.e. a reactor packed with a mixture of crude oil, sand, clay, and water, which is heated externally to follow a programmed heating rate. Air is injected at a constant flow rate (F_{in}) to react with the oil sample. The products are combustion gases (F_{out}) and residual solid.

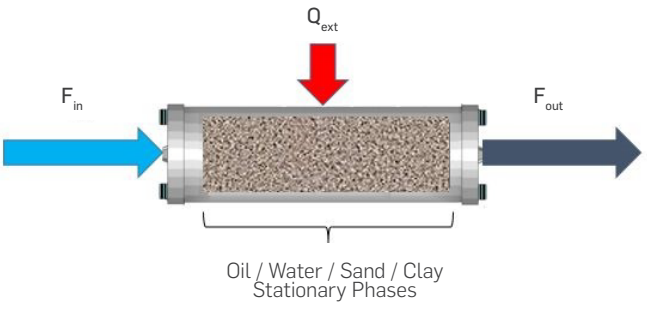

Figure 1. Schematic diagram for a kinetic cell experiment.

The kinetic cell was modeled as a spatially homogeneous, semi-batch reactor, adapted to account for porous media where only gas flows through the reactor, and the oil and solid phases are stationary. This is an approximation that does not consider the effect of gravity on the liquid or gas flow. As this model was used to understand the effect of gas-phase chemistry, this approach will have a minor effect on the model predictions. Oil and water are considered immiscible. Diffusion transport was neglected because of the typically high Peclet numbers of reservoir flows as mentioned by Kristensen [13]. Equation 1 shows the mole balance of species i in the kinetic cell.

$$\frac{dN_i}{dt} = \sum_j F_{i,j}^{in} - \sum_j F_{i,j}^{out} + \sum_r \Lambda^{i,r}\gamma^{i,r} \tag{1}$$

where N_i represents the number of moles of species i in the porous medium, F_{ij}^{in} and F_{ij}^{out} are, respectively, the inlet and outlet molar flow rates of species i in phase j, $\Lambda^{i,r}$ and $\gamma^{i,r}$ are, respectively, the stoichiometric coefficient and reaction rate for species i in reaction r.

ONE-DIMENSIONAL REACTOR

In the model for the One-dimensional reactor considered convective transport in porous media, diffusion is neglected. In Figure 2, a sum of perfectly mixed reactors in series represents the flow in a 1D reactor. The mole balance from Equation 1 is solved for each reactor. The inlet for reactor K corresponds to the outlet from reactor *k-1*; the outlet from reactor *k* is the inlet for reactor *k+1*.

Considering oil and solid phases stationary, and that only gas flows through the reactor, the One-dimensional reactor module in the simulation tool is suitable for modeling ramped temperature oxidation (RTO) experiments.

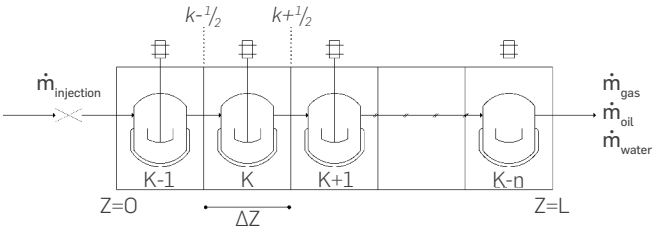

Figure 2. Schematic diagram for the discretization used for the One-dimensional reactor and the Combustion tube. $\dot{m}_{oil}$ and $\dot{m}_{water}$ apply only for the Combustion tube

COMBUSTION TUBE

The Combustion tube module considers oil, gas, and water flow as shown in Figure 2. Equation 2 presents the mole balance of species i in phase j.

$$\frac{\partial}{\partial t}(C_i) = \frac{\partial}{\partial t}\left(\sum_j \rho_j \phi S_j y_{i,j}\right) = -\nabla \cdot \left(\sum_j \rho_j u_j y_{i,j}\right) + \hat{q}_i \tag{2}$$

where C_i is the concentration of species i, ρ_j is the molar density for phase j, ϕ is the porosity, S_j is the saturation of phase j, $y_{i,j}$ is the molar fraction of species i in phase j, u_j is the velocity of phase j, and $\hat{q}_i$ is the generation rate of the species i. Equation 2 is solved for each species for all phases using a fine finite volume method.

The velocity of the fluid phases was represented by Darcy's equation (Equation 3).

$$u_j = -\frac{k_{rj}}{\mu_j}\mathbf{k}\left(\nabla P_j - \rho_j g \nabla D\right) \tag{3}$$

where P_j is the pressure for phase j, k is the permeability tensor, k_{rj} is the relative permeability of phase j, μ_j is the dynamic viscosity of phase j, and D is the bed depth in the direction of the gravity vector. The pressure gradient was approximated using a central difference scheme.

Equation 4 presents the energy balance where U_r is the internal energy of the porous media, U_j is the internal energy of phase j, α is the thermal conductivity of the porous media, and $\hat{q}_{h,i}$ is the heat generated by chemical reactions. The reactor was considered in adiabatic operation.

$$\frac{\partial}{\partial t}\left((1-\phi)U_r + \phi\sum_{j=1}^{np}\rho_j S_j U_j\right) + \nabla \cdot \sum_{j=1}^{np}\rho_j S_j U_j + \nabla \cdot (-\alpha \nabla T) = \hat{q}_{h,i} \tag{4}$$

Closure of the system of equations for multiphase flow is given by Equation 5 that involves an equation of state that bounds the evolution of mass and energy.

Table 1. Kinetic parameters used in the simulations [15].

Reaction	KINETIC CELL - PFR		COMBUSTION TUBE		
	Frequency factor $\left[\frac{1}{min \times kPa}\right]$	Activation energy $\left[\frac{J}{mol}\right]$	Frequency factor $\left[\frac{1}{min \times kPa}\right]$	Activation energy $\left[\frac{J}{mol}\right]$	Reaction enthalpy $(-\Delta H_i)\left[\frac{J}{mol}\right]$
R. 1	2.072×10^2	6.356×10^4	1.000×10^{-2}	2.256×10^4	8.78×10^5
R. 2	5.525×10^2	8.753×10^4	2.500×10^2	6.753×10^4	7.04×10^6
R. 3	6.907×10^2	9.758×10^4	2.200×10^2	8.758×10^4	7.04×10^6

$$\left(\hat{c}_R(1-\phi)+\phi\hat{c}_f\right)\frac{\partial P^k}{\partial t}=\phi\hat{c}_T\frac{\partial T^k}{\partial t}+\frac{1}{V_b}\sum_{i=1}^{nc}\frac{\partial V_P}{\partial N_i}\frac{\partial N_i^k}{\partial t} \quad (5)$$

where $\hat{c}_R$ is the rock compressibility, $\hat{c}_f$ is the average fluid compressibility, and $\hat{c}_T$ is the thermal expansion coefficient. Phase equilibrium was represented through a five-parameter correlation for the K-value as further explained in [34]

REACTION SCHEME

As stated above, all gas phase reactions were represented by the GRI-Mech 3.0 chemical mechanisms [32]. While multiple studies [1,12,15,35–38] have been conducted to understand oil reactivity during ISC, few present the detailed information (exact reactor dimensions, kinetic parameters, transport, and thermophysical properties) required for the evaluation of simulation tools. One exception is the thesis of Bazargan [15], which provides all the details necessary for attempting validation of a simulation tool. Therefore, the reaction scheme from R1 to R3, proposed in [15], was used in all the simulations below. Through this paper, the term "reaction scheme" is preferred vs. "reaction mechanism", as the latter seems more suitable for cases where actual chemical species participate in the reactions. The use of pseudo-species, such as "Oil", "Coke1", and "Coke2", motivated by the large number of molecules present in the system, makes the term "reaction scheme" more appropriate.

$$Oil + 4.24\ O_2 \rightarrow\ 0.36\ Coke_1 \quad (R1)$$

$$Coke_1 + 33.8\ O_2 \rightarrow 6.86\ Coke_2 + 19.77\ CO_2 + 29.06\ CO + 22 H_2O \quad (R2)$$

$$Coke_2 + 12.29\ O_2 \rightarrow 9.21\ CO_2 + 6.161\ CO + 8\ H_2O \quad (R3)$$

Reactions R1 to R3 represent, respectively, the cracking, low-temperature oxidation (LTO), and high-temperature oxidation (HTO) stages. Although this short-reaction scheme was selected to reduce computational time, the simulation tool accepts more complex reaction schemes. No attempt was made to improve the kinetic scheme as it was selected only to illustrate the abilities of the Simulation toolbox. Table 1 presents the kinetic parameters, taken from reference [15].

3. RESULTS AND DISCUSSION

The following sections illustrate the use of the different components of the simulation tool with real applications to ISC experiments. The first example evaluates the existence of gas phase reactions during ISC. A second example demonstrates the presence of concentration gradients in kinetic cells. The third and fourth examples involve, respectively, the evaluation of pressure changes and ignition in combustion tubes.

KINETIC CELL - ANALYSIS OF REACTIONS IN THE GASEOUS PHASE

For the validation of the kinetic cell module, Table 2 presents the conditions that were used to simulate the RTO experiment. The oil used was that described by Dechelette et al. [37], and the relevant properties were exactly those reported in [15]. Figure 3 compares the results of the simulation with those in the referred literature. Both for LTO (T < 400°C) and HTO reactions (T > 400°C), the match is quite good.

Table 2. Simulation input for the experiment in reference [15].

Parameter	Value
Pressure	689 kPa
Air flow (STP)*	0.42 mol/min
Reactor Volume	3.0×10^{-5} m^3
Oil molecular weight	538 g/mol
Initial temperature	298 K
Diameter	3.1 cm
Length	12.0 cm
Initial oil in place	2.0 g
Length of porous media with oil	4.0 cm
Heating rate	3 °C/min

*STP: standard pressure (101325 Pa) and temperature (298 K)

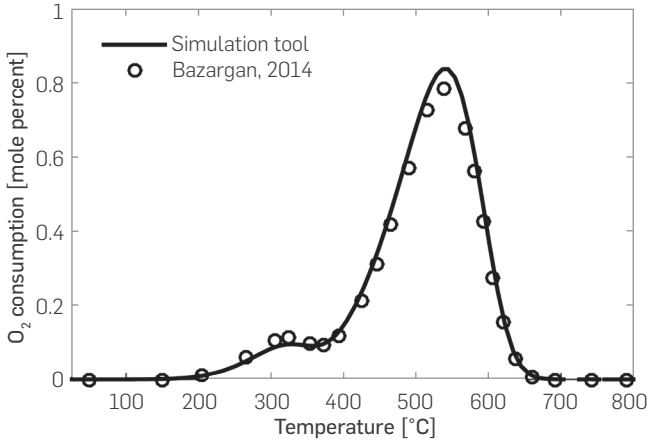

Figure 3. Oxygen consumption profile. Comparison between simulation tool (solid line) and Bazargan [15] (circles).

Once the validation was completed, and to illustrate the capabilities of the Kinetic cell module, the importance of the gas-phase CO oxidation reaction during ISC was addressed. While the effect of other gas phase reactions, such as those that involve water and other hydrocarbons in the vapor phase, would be of interest for the application of ISC, the scope of the present research is to demonstrate the toolbox ability to deal with complex kinetic schemes; therefore, this study only deals with CO oxidation. With few exceptions [39–41] in the referred literature, ISC has been described as an exclusively heterogeneous process. However, the existence of gas-phase oxidation reactions may be a matter of concern given the relatively high temperatures, particularly of HTO, the high concentration of gas-phase hydrocarbons, and the presence of oxygen in some regions of the process. An option for modeling gas phase reactions is, therefore, a desirable feature of any simulation tool for ISC.

In the illustrative simulations of the Kinetic cell module, the thermophysical properties and simulation parameters were those used in the validation, but the diameter of the reactor was 1.27 cm, the oxidizer flow rate was 300 mL (STP)/min with a composition (molar fraction) of O_2: 0.21, H_2O: 0.001, and N_2: 0.789. The presence of water in the oxidizer stream is to be noted, given the well-known importance of the hydroxyl radical (OH*) on carbon monoxide oxidation mentioned by Winter [42–44]. While the evaluation of the effect of water vapor on the system was beyond the scope of the paper, the Simulation toolbox can easily account for different water vapor concentrations. The heating rate was 30°C/min until 800°C. At this temperature, isothermal operation started. The initial gas saturation was fixed at 0.9, while oil saturation was 0.1.

Figure 4 compares the predictions for the molar fractions of major combustion species (O_2, CO_2, and CO) when only heterogeneous reactions are considered with those when gas phase reactions are also simulated. At temperatures higher than 700°C, CO oxidation in the gas phase becomes important, as the CO concentration is lower than that observed when only heterogeneous reactions take place. Furthermore, carbon dioxide increases as it is the final product of CO oxidation. Although not so evident, oxygen concentration also decreases due to the activation of the homogeneous phase when the temperature is higher than 700°C.

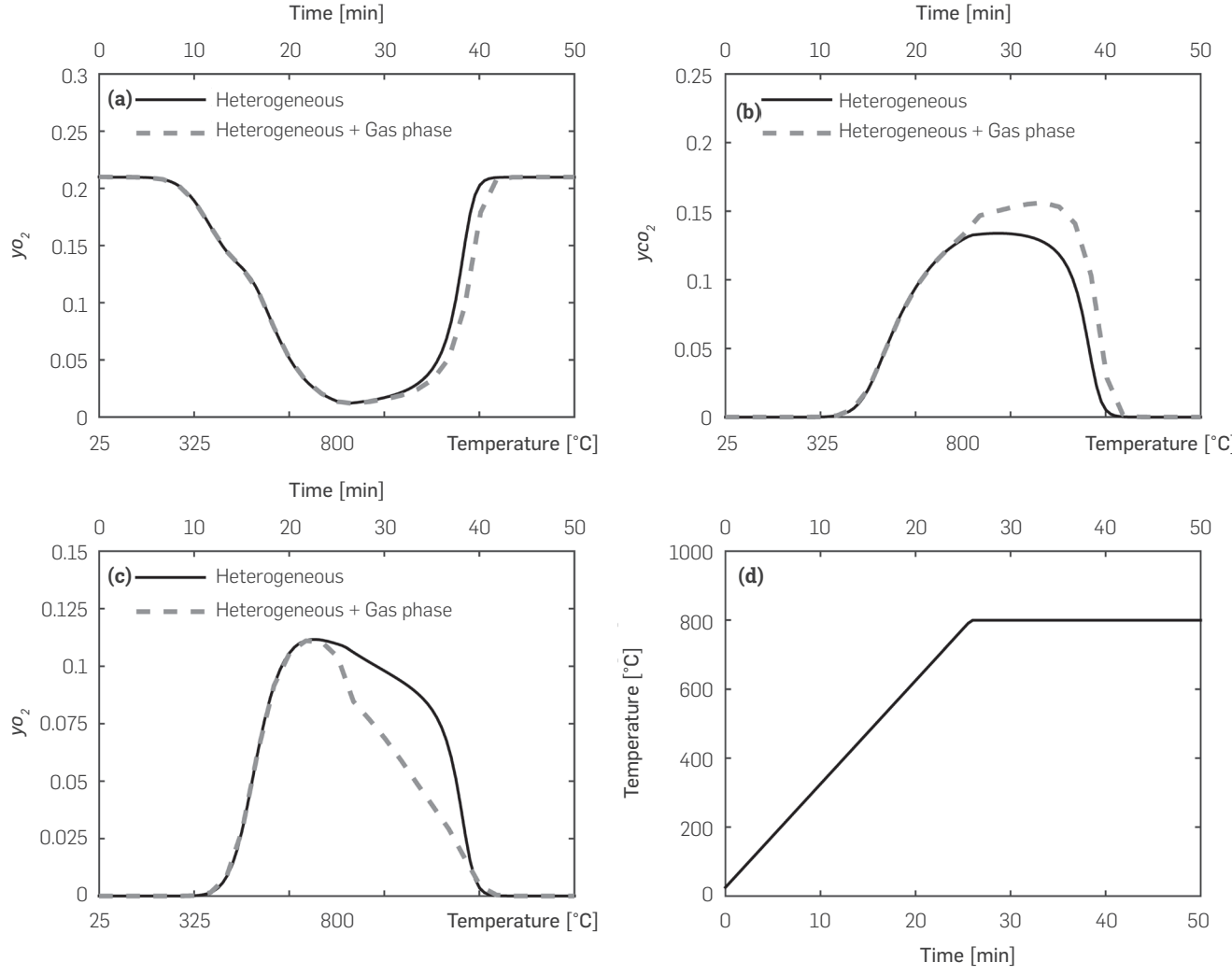

Figure 4. Predicted variation of major combustion species during a RTO-isothermal experiment. Results obtained with the kinetic cell module considering heterogeneous and heterogeneous + gas phase reaction.

The second set of illustrative simulations for the Kinetic cell module evaluated more in depth the effect of temperature on the homogeneous oxidation of CO when the volumetric injection rate of air was 700 mL (STP)/min and the oil and gas compositions were the same as those used in the simulations shown in Figure 4. The saturation of gas, water, and oil were set as 0.79, 0.05, and 0.16, respectively. Figure 5 presents the isocontours of oxygen (Figure 5a) and carbon monoxide (Figure 5b) mole fractions, and the log of the reaction rate of CO consumption (Figure 5c) as a function of the time and temperature of the experiment. This plot is the result of multiple isothermal simulations, each one at a different temperature. In Figure 5b, a vertical line at 700°C represents an isothermal simulation that predicts that the highest CO concentration is 0.1 (mole fraction) when the time varies between 2 and 7 minutes and the combustion ends after 24 min when the oxygen and CO molar fractions regain the input values of 0.21 and 0.0, respectively, and the log of the rate of CO consumption is below 10^{-7} $kmol/m^3s$. Figure 5 shows that, at conditions relevant to the ISC experiments in Table 2 that are for heavy oil, CO oxidation can take place in the gaseous phase. The extent of the oxidation depends on the temperature and oxygen concentration in the system. In Figure 5, CO oxidation is significant at temperatures above 700°C. It is worth noting that the analysis above was at 689 kPa as the experimental data in [15] was at those conditions. While the effect that pressure changes would have on homogeneous reactions is out of the scope of this research, we consider that the ability of the simulation toolbox proposed that the use of complex chemical schemes would be very useful as one could anticipate that heterogeneous chemistry, i.e. gas/liquid and gas/solid reactions, as well as gas-phase reactions, will be more active given the larger number of molecular collisions derived from a higher pressure.

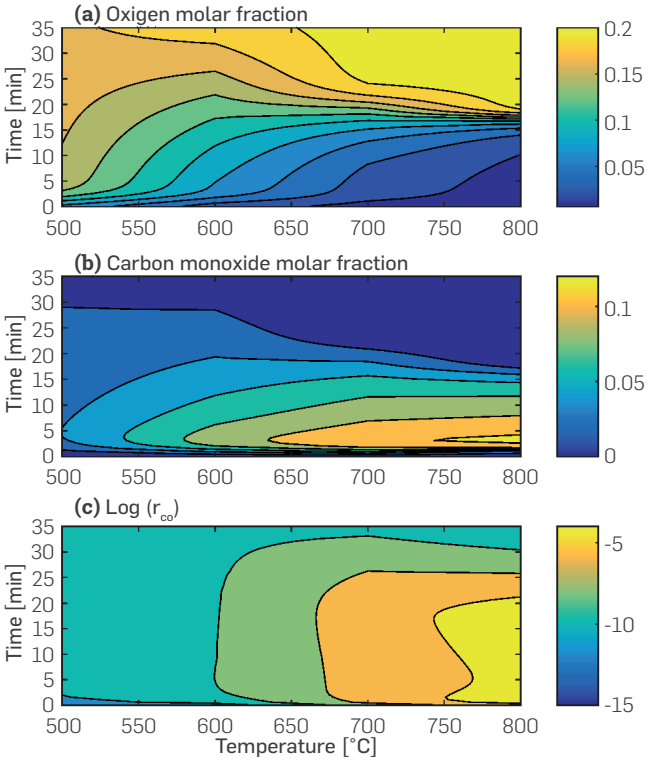

Figure 5. Predicted concentration of a) O_2 and b) *CO*, and c) log reaction rate of *CO* during isothermal experiments of ISC of crude oil. Results obtained with the kinetic module considering heterogeneous and gas phase reactions.

ONE-DIMENSIONAL REACTOR - KINETIC CELL WITH AXIAL GRADIENTS

While kinetic cells have been traditionally modeled as homogeneous systems, recent studies have cast doubt on the validity of that approach [19]. The One-dimensional reactor module, described above, is particularly suitable for the analysis of ISC experiments where axial concentration or temperature gradients may be present, but where oil flow can be neglected. In the simulations, the oxidizer (21% v/v O_2, N_2 balance) had a volumetric flow of 100 mL (STP)/min. The heating rate was 5 °C/min until 800°C, where isothermal operation was maintained. The initial gas and oil saturations were 0.75 and 0.25, respectively. The pressure was constant (1.01MPa).

Figure 6 shows the oxygen molar fraction as a function of distance in the cell and time. When the temperature is 300°C, the oxidation reactions become significant, and oxygen decreases almost to zero at the exit of the Kinetic cell. After that, all the oxygen injected is consumed by the remaining oil in the kinetic cell. Towards the end of the simulation, when the temperature is stable at 800°C, the oxygen concentration is not fully depleted in the cell.

Figure 7 presents the data in Figure 6 but in such way that each line corresponds to a constant temperature in Figure 6. At temperatures below 425°C (Figure 7a), the reaction rates are moderate and the oxygen in the system is above zero along the reactor. When the temperature reaches 625°C or higher, Figure 7b, a sigmoidal curve forms as oxygen is completely depleted close to the end of the reactor.

The profiles of oil saturation in Figure 8, show that at low temperatures, oil is present throughout the cell. On the contrary, at temperatures above 425°C, oil is consumed at the entrance of the Kinetic cell and the reaction occurs in a combustion front.

Clearly, under these conditions, the simulation shows that the combustion in the kinetic cell is not homogeneous. Different strategies such as higher oxidizer flow or lower oil saturation can control gradients inside the cell, as described by Lopez [19]. As demonstrated with this example, the One-dimensional module can help in designing experiments that guarantee a homogeneous concentration in the cell and facilitate the extraction of kinetic parameters from the experimental data as one can add an optimization routine that uses the Simulation toolbox to determine the kinetic parameters.

COMBUSTION TUBE - PRESSURE ANALYSIS

The use of the Combustion tube module is illustrated through validation against simulations with the physical STARS modeling tools as a means to verify the model response. The simulations considered a volumetric flow of air of 10 L (STP)/min entering the system at 500°C to secure ignition; the medium had a permeability of 10 Darcy and an oil saturation of 0.05. The crude had an API of 8.9 and the variation of viscosity with temperature was that described in [15]. A more detailed description of all the relevant oil properties, as well as all the inputs to STARS is given in [34]. Figure 9 shows the comparison of the results obtained with the simulation tool and those of STARS for two different simulation times. The match is almost perfect for temperature, pressure, and oxygen mole fraction. It should be noted, however, that the conditions of the simulation of the combustion tube are far from those observed in the field, and

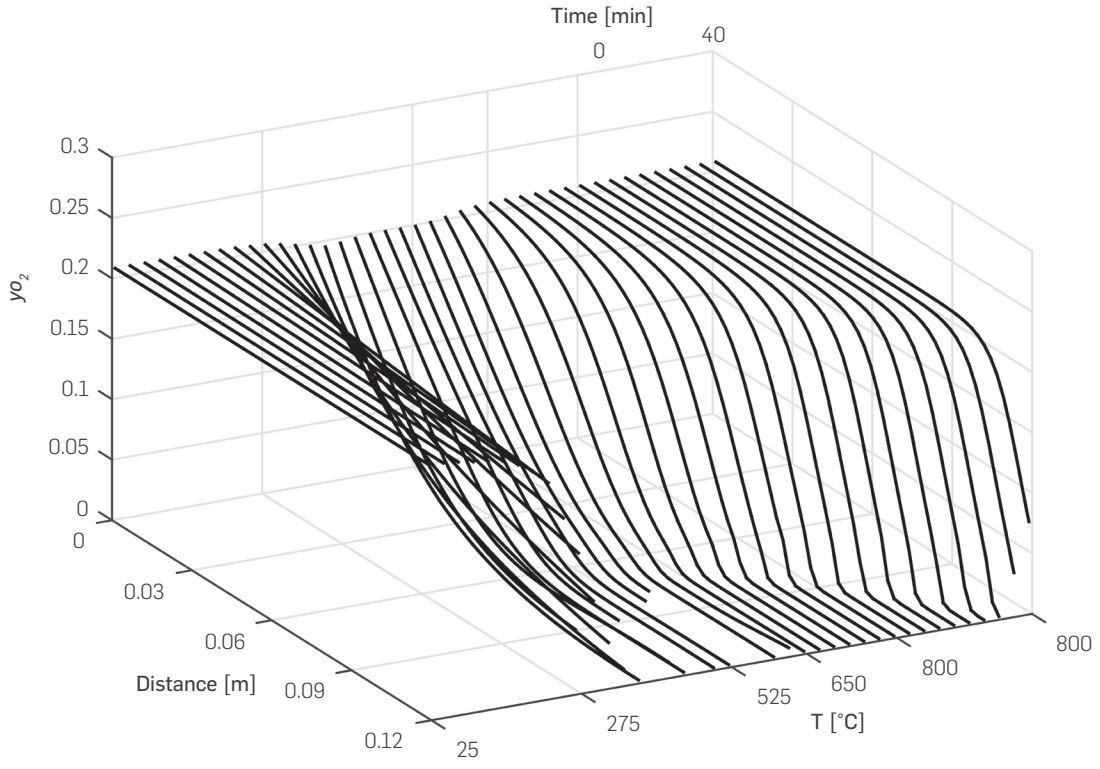

Figure 6. Predicted variation of oxygen mole fraction for a 5°C/min RTO experiment using the One-dimensional module.

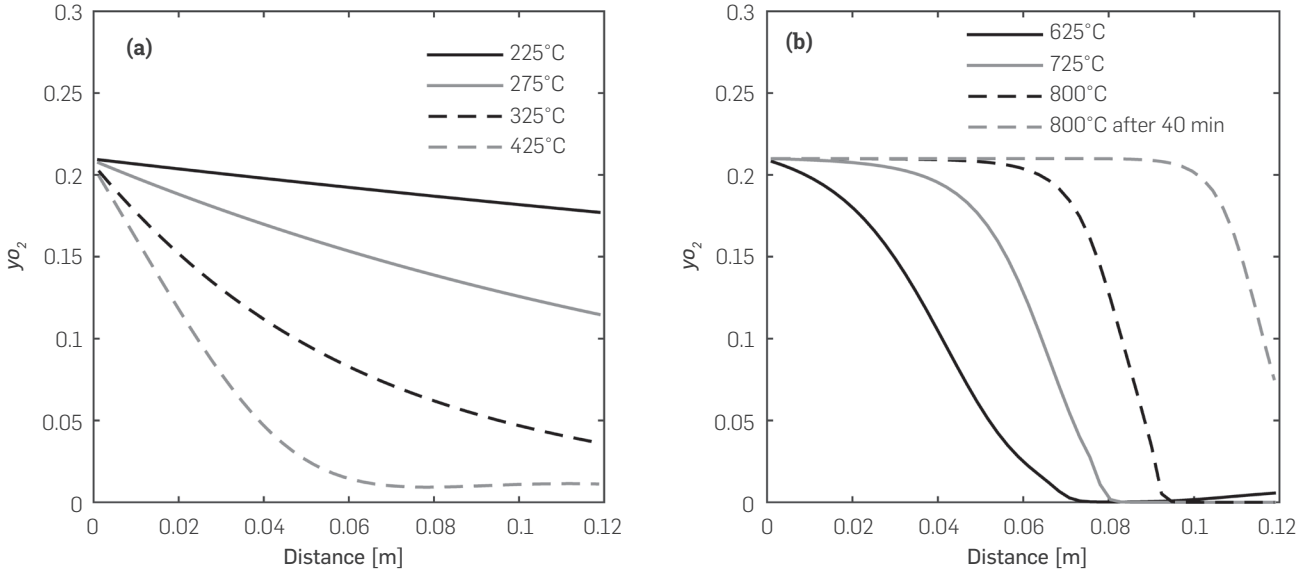

Figure 7. Predicted variation of the oxygen molar fraction along the reactor at different temperatures for the RTO experiment. a) T < 425°C. b) T > 625°C

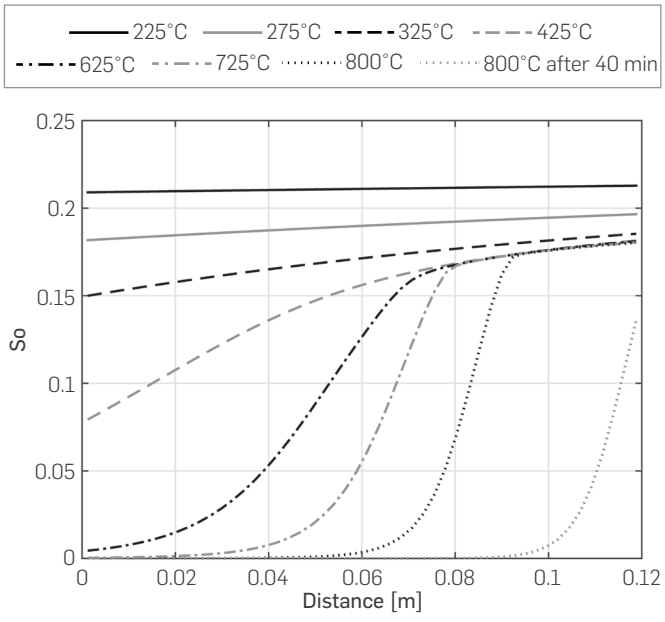

Figure 8. Predicted oil saturation profile along the reactor for different temperatures with the One-dimensional module

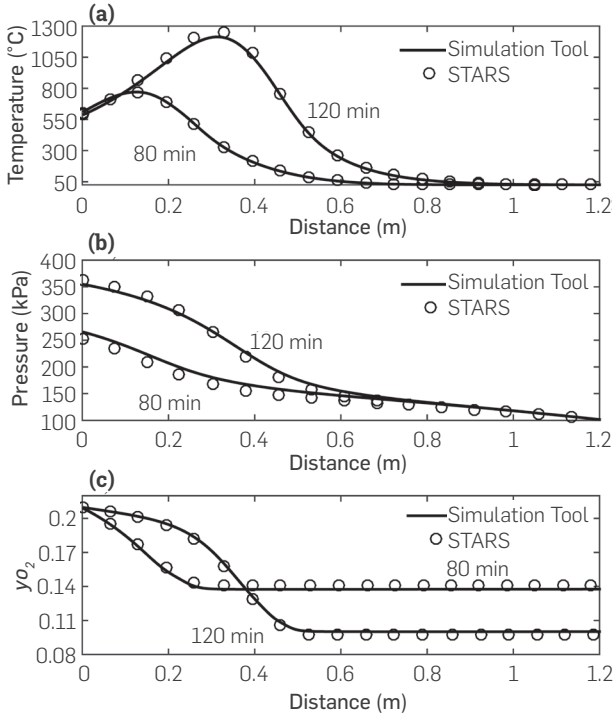

Figure 9. Combustion tube module validation with STARS [24]. a) Temperature profile, b) pressure profile, c) Oxygen mole fraction.

the pressure is lower, the permeability is high, and the oil saturation is lower than that typically observed in the reservoirs. These values, nonetheless, are common in ISC combustion experiments, such as those that the Simulation toolbox here proposed to simulate.

The advantage of the Combustion tube module in the simulation tool described in this paper, when compared with traditional reservoir physical modeling tools, is that it can be easily coupled with different reaction mechanisms, including gas-phase chemistry, as was described in the kinetic cell section. Thus, emphasis can be made in the evaluation of the kinetic parameters.

COMBUSTION TUBE – IGNITION

A second illustrative example of the Combustion tube module simulated a regular combustion tube experiment with electrical heating for ignition. The experimental conditions were the same as those in the previous section. The initial oil saturation was 0.2. The initial pressure and temperature were 101.13 kPa and 25°C, respectively. The heating rate was set as 20°C/min for 30 minutes in the first 0.10 m of the tube, to obtain ignition, after adiabatic conditions were defined, so that a self-sustained process was maintained.

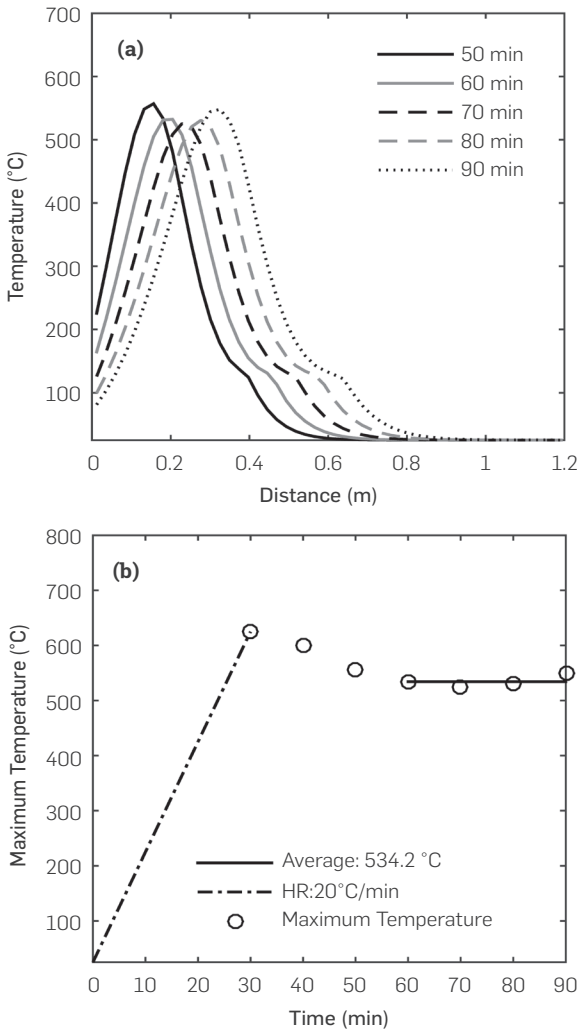

Figure 10. Temperature profiles. a) Combustion tube process b) Temperature Control Monitoring.

The temperature profiles in Figure 10a show how the combustion front, the place where the temperature is the highest at a specific time, advances through the porous media. A steam plateau, a region downstream of the combustion front where temperature reaches a value of around 120°C, is also evident. The propagation of the combustion front is stable through the duration of the simulation.

Figure 10b shows the variation of maximum temperature with time. The dashed line, which shows a linear increase of temperature over time, corresponds to the ignition process when the heating rate is set to 20°C/min in the first 0.1 m of the reactor. Thirty minutes after ignition, the temperature reaches a pseudo-steady state at an average value of 534°C. This value is of the order of those reported in ISC experiments [27,29,45,46].

CONCLUSIONS

This study described a simulation tool that can be used to study the experimental results obtained in laboratory-scale ISC experiments. Through three stand-alone modules: Kinetic cell, One-dimensional reactor, and Combustion tube, which share common thermodynamic and transport databases and chemical schemes, the kinetic can be easily tested under different experimental conditions. This ability can be used to obtain more comprehensive simulation parameters, which can be applied to reservoir physical modeling tools.

The simulation tool is unique in its ability to integrate homogeneous phase reactions in the analysis of ISC experiments. It also clearly states the equations used in the simulation. This last characteristic is particularly suitable to understand the effect of the model on the evaluation of experimental data.

Four examples selected to illustrate the simulation tool indicate that, while all modules reproduced as expected, typically-documented ISC behavior, the inclusion of homogeneous chemistry suggests that the production of carbon monoxide is very sensitive to operating conditions, particularly to O_2 and CO partial pressures and temperature. The simulations show that changes in the CO concentration due to the gas-phase oxidation occur even at 700°C and 689 kPa. This result must be confirmed with experiments in future studies to determine the impact that the gas-phase reaction and concentration gradients would have on the evaluation of kinetic parameters for ISC.

The one-dimensional reactor module can be used to evaluate strategies to prevent significant concentration gradients in a kinetic cell and, thus, simplify the evaluation of chemical parameters from experimental data. The Combustion tube module captures ISC combustion characteristics such as oil ignition with external heaters and the advance of the reaction front.

ACKNOWLEDGEMENTS

We highlight the financial support from "Jóvenes investigadores, convocatoria 566 de 2012" and the project of Colciencias-Ecopetrol "Caracterización Mediante Técnicas Láser de las Reacciones Químicas de Petróleo Crudo Durante Combustion In-Situ" with contract RC. No. 0264-2013.

REFERENCES

1. Khansari, Z., Kapadia, P., Mahinpey, N., & Gates, I. D. (2014). A new reaction model for low temperature oxidation of heavy oil: Experiments and numerical modeling. *Energy*, 64, 419–428. https://doi.org/10.1016/j.energy.2013.11.024

2. Alpak, F. O., Vink, J. C., Gao, G., & Mo, W. (2013). Techniques for effective simulation, optimization, and uncertainty quantification of the in-situ upgrading process. *Journal of Unconventional Oil and Gas Resources*, 3–4(October), 1–14. https://doi.org/10.1016/j.juogr.2013.09.001

3. Dong, X., Liu, H., Chen, Z., Wu, K., Lu, N., & Zhang, Q. (2019). Enhanced oil recovery techniques for heavy oil and oilsands reservoirs after steam injection. *Applied Energy*, 239(January), 1190–1211. https://doi.org/10.1016/j.apenergy.2019.01.244

4. Nesterov, I., Shapiro, A., & Stenby, E. (2013). Numerical analysis of a one-dimensional multicomponent model of the in-situ combustion process. *Journal of Petroleum Science and Engineering*, 106, 46–61. https://doi.org/10.1016/j.petrol.2013.03.022

5. Zhu, Z. (2011). *Efficient simulation of thermal enhanced oil recovery process* (Issue August). Stanford University.

6. Rodriguez, J. R. (2004). *Experimental and analytical study to model temperature profiles and stoichiometry in oxigen enriched in situ combustion*. Texas A & M University.

7. Sarathi, P. S. (1999). In Situ Combustion Handbook - Principles and Practice. In *Combustion*. National Petroleum Technology Office U. S. DEPARTMENT OF ENERGY. https://doi.org/10.2172/3175

8. Cazarez-Candia, O., & Centeno-Reyes, C. (2009). Prediction of Thermal Conductivity Effects on in-situ Combustion Experiments. *Petroleum Science and Technology*, 27(14), 1637–1651. https://doi.org/10.1080/10916460802608958

9. Coats, K. (1980). In-Situ Combustion Model. *SPE Journal*, 20(6), 533–554. https://doi.org/https://doi.org/10.2118/8394-PA

10. Dean, R. H., & Lo, L. L. (1988). Simulations of Naturally Fractured Reservoirs. SPE International, Society of *Pretroleum Engineers*, 3(02), 638–648. https://doi.org/https://doi.org/10.2118/14110-PA

11. Turta, A. (2013). In Situ Combustion. In James J.Sheng (Ed.), *Enhanced Oil Recovery Field Case Studies* (pp. 447–542). Elsevier Inc. https://doi.org/10.1016/B978-0-12-386545-8.00018-X

12. Lapene, A., Debenest, G., Quintard, M., Castanier, L. M., Gerritsen, M. G., & Kovscek, A. R. (2011). Kinetics oxidation of heavy oil. 1. Compositional and full equation of state model. *Energy and Fuels*, 25(11), 4886–4896. https://doi.org/10.1021/ef200365y

13. Kristensen, M. R. (2008). *Development of Models and Algorithms for the Study of Reactive Porous Media Processes*. Technical University of Denmark.

14. Chen, B., Castanier, L. M., & Kovscek, A. R. (2014). Consistency Measures for Isoconversional Interpretation of In-Situ Combustion Reaction Kinetics. *Energy & Fuels*, 28(2), 868–876. https://doi.org/10.1021/ef4020235

15. Bazargan, M. (2014). *Measurement of in-situ combustion reaction kinetics with high fidelity and consistent reaction upscaling for reservoir simulation*. Stanford University.

16. Bazargan, M., Lapene, A., Chen, B., Castanier, L. M., & Kovscek, A. R. (2013). An induction reactor for studying crude-oil oxidation relevant to in situ combustion. *Review of Scientific Instruments*, 84(7). https: An induction reactor for studying crude-oil oxidation relevant to in situ combustion //doi.org/10.1063/1.4815827

17. Belgrave, J., Moore, R., Ursenbach, M., & Bennion, D. (1993). A comprehesive approach to in situ combustion modeling. *SPE Advance Technology Series*, 1(1), 98–107. https://doi.org/10.2118/20250-PA

18. Moore, R. G., Ursenbach, M. G., Laureshen, C. J., Belgrave, J. D. M., & Mehta, S. A. (1999). Ramped Temperature Oxidation Analysis of Athabasca Oil Sands Bitumen. *Journal of Canadian Petroleum Technology*, 38(13), 1–10. https://doi.org/10.2118/99-13-40

19. López, S., & Molina, A. (2017). Criteria to Select Operational Variables That Improve the Accuracy of the Evaluation of Kinetic Parameters in a Kinetic Cell Used in the Study of in Situ Combustion. *Energy and Fuels*, 31(3), 2390–2397. https://doi.org/10.1021/acs.energyfuels.6b02191

20. Liu, D., Tang, J., Zheng, R., & Song, Q. (2020). Influence of steam on the coking characteristics of heavy oil during in situ combustion. *Fuel*, 264(September 2019), 116904. https://doi.org/10.1016/j.fuel.2019.116904

21. Kristensen, M. R., Gerritsen, M. G., Thomsen, P. G., Michelsen, M. L., & Stenby, E. H. (2008). An Equation-of-State Compositional In-Situ Combustion Model: A Study of Phase Behavior Sensitivity. *Transport in Porous Media*, 76(2), 219–246. https://doi.org/10.1007/s11242-008-9244-6

22. Kee, R. J., Rupley, F. M., Miller, J.A., Coltrin, M.E., Grcar, J. F., Meeks, E., Moffat, H. K., Lutz, A. E., Dixon-Lewis, G., Smooke, M. D., Warnatz, J., Evans, G.H., Larson, R. S., Mitchell, R. E., Petzold, L. R., Reynolds, W. C., Caracotsios, M., Stewart, W. E., Glarborg, P., Wang, C., & Adigun, O. (2013). *Chemkin collection, Reaction Design, Inc.*,. Reaction Design, Inc.,.

23. Goodwin, D. G., Moffat, H. K., & Speth, R. L. (2016). *Cantera: An Object-oriented Software Toolkit for Chemical Kinetics, Thermodynamics, and Transport Processes*.

24. CMG. (2010). *Advanced Process and Thermal Reservoir Simulator STARS*. Computer Modelling Group.

25. Schlumberger. (2010). *ECLIPSE Industry-Reference Reservoir Simulator Black oil, compositional, thermal, and streamline reservoir simulation*.

26. Lie, K., Krogstad, S., Ligaarden, I. S., Natvig, J. R., Nilsen, H. M., & Skaflestad, B. (2012). Open-source MATLAB implementation of consistent discretisations on complex grids. *Computational Geosciences*, 16(2), 297–322. https://doi.org/10.1007/s10596-011-9244-4

27. Yang, X., & Gates, I. D. (2009). Combustion Kinetics of Athabasca Bitumen from 1D Combustion Tube Experiments. *Natural Resources Research*, 18(3), 193–211. https://doi.org/10.1007/s11053-009-9095-z

28. Liu, Z., Jessen, K., & Tsotsis, T. T. (2011). Optimization of in-situ combustion processes: A parameter space study towards reducing the CO2 emissions. *Chemical Engineering Science*, 66(12), 2723–2733. https://doi.org/10.1016/j.ces.2011.03.021

29. Oliveros, L. R., Yatte, F. C., Bottia Ramirez, H., & Munoz Navarro, S. F. (2013). Design Parameters And Technique Evaluation Of Combustion Processes From Tube Testing. *SPE Heavy Oil Conference-Canada*, 25. https://doi.org/10.2118/165458-MS

30. ANSYS. (2016). *ANSYS Fluids - CFD Simulation Software, Academic Research*.

31. OpenFOAM. (2016). *OpenFOAM®- The Open Source Computational Fluid Dynamics* (CFD) Toolbox. OpenCFD Ltd.

32. Gregory P. Smith, David M. Golden, Michael Frenklach, Nigel W. Moriarty, Boris Eiteneer, Mikhail Goldenberg, C. Thomas Bowman, Ronald K. Hanson, Soonho Song, William C. Gardiner, Jr., Vitali V. Lissianski, Z. Q. (n.d.). *GRI-MECH 3.0*.

33. Modeling, C. (n.d.). *http://creckmodeling.chem.polimi.it/menu-kinetics*.

34. Hincapie A, J. F. (2016). *Simulation toolbox for in-situ combustion applied to experimental setups*. Universidad Nacional de Colombia Sede Medellín Facultad de Minas.

35. Chen, B. (2012). *Investigation of in-situ combustion kinetics using the isoconventional principle*. Stanford University.

36. Cinar, M. (2011). *Kinetics of crude-oil combustion in porous media interpreted using isoconversional methods*. Stanford University.

37. Dechelette, B., Christensen, J. R., Heugas, O., Quenault, G., & Bothua, J. (2006). Air injection - Improved determination of the reaction scheme with ramped temperature experiment and numerical simulation. *Journal of Canadian Petroleum Technology*, 45(1), 41–47. https://doi.org/10.2118/06-01-03

38. Burger, J. G., & Sahuquet, B. C. (1972). Chemical Aspects of in-Situ Combustion - Heat of Combustion and Kinetics. *Society of Petroleum Engineers of AIME Journal*, 12(5), 410–422. https://doi.org/10.2118/3599-PA

39. Hoekstra, B. E. (2011). *Impact of chemical reactions in the gas phase on the in-situ combustion process: An experimental study*. TU Delft.

40. Khoshnevis Gargar, N., Achterbergh, N., Rudolph-Floter, S., & Bruining, H. (2010). In-Situ Oil Combustion: Processes Perpendicular to the Main Gas Flow Direction. *Proceedings of SPE Annual Technical Conference and Exhibition*. https://doi.org/10.2118/134655-MS

41. Ochoa, D. V. (2018). *Efecto de las reacciones químicas, en fase gaseosa, sobre la producción de monóxido de carbono, durante la combustión in situ*. Universidad Nacional de Colombia - Sede Medellín.

42. Winter, F., Wartha, C., Löffler, G., & Hofbauer, H. (1996). The NO and N2O formation mechanism during devolatilization and char combustion under fluidized-bed conditions. *Proc. Comb Inst*, 26(2), 3325–3334. https://doi.org/10.1016/S0082-0784(96)80180-9

43. Winter, F., Löffler, G., Wartha, C., Hofbauer, H., Preto, F., & Anthony, E. J. (1999). The NO and N2O Formation Mechanism under Circulating Fluidized Bed Combustor Conditions: from the Single Particle to the Pilot-Scale. *The Canadian Journal of Chemical Engineering*, 77(2), 275–283. https://doi.org/10.1002/cjce.5450770212

44. Winter, F., Wartha, C., & Hofbauer, H. (1999). Relative importance of radicals on the N2O and NO formation and destruction paths in a quartz CFBC. Journal of Energy Resources Technology, *Transactions of the ASME*, 121(2), 131–136. https://doi.org/https://doi.org/10.1115/1.2795068

45. Moore, R. G., Laureshen, J., Ursenbach, M. G., & Mehta, S. A. (1995). In Situ Combustion Reservoirs in Canadian Heavy Oil. *Fuel*, 74(8), 1169–1175. https://doi.org/10.1016/0016-2361(95)00063-B

46. Sibbald, L., Moore, A. G., Bennion, D. W., Chmilar, B. J., & Ursenbach, M. G. (1988). In Situ Combustion Experimental Studies Using A Combustion Tube System With Stressed Core Capability. *Annual Technical Meeting*, 19. https://doi.org/10.2118/88-39-60

AUTHORS

Juan Felipe Hincapie Alvarez
Affiliation: Universidad Nacional de Colombia, Medellín, Colombia
ORCID: https://orcid.org/0000-0001-7804-2292
e-mail: jufhincapieal@unal.edu.co

Sebastian Lopez Gomez
Affiliation: Universidad Nacional de Colombia, Medellín, Colombia
ORCID: https://orcid.org/0000-0002-0369-7187
e-mail: selopezgo@unal.edu.co

Alejandro Molina Ochoa
Affiliation: Universidad Nacional de Colombia, Medellín, Colombia
ORCID: https://orcid.org/ 0000-0002-0710-9418
e-mail: amolinao@unal.edu.co

How to cite: Hincapie, J. F., López, S., Molina, A. (2022). Simulation tool for the analysis of in-situ combustion experiments that considers complex kinetic schemes and detailed mass transfer- theoretical analysis of the gas phase co oxidation reaction. *CT&F - Ciencia, Tecnología & Futuro*, 12(1), 95-106. https://doi.org/10.29047/01225383.402

NOMENCLATURE

F_i	Molar flow rate	mol • min^{-1}
N_i	Amount of moles	mol
$\Lambda^{i,r}$	Stoichiometric matrix	
γ^r	Reaction rate	mol • min^{-1}
m_i	Amount of mass	g
t	Time	min
C_i	Concentration	mol • m^{-3}
ρ_j	Phase molar density	mol • m^{-3}
ϕ	Porosity	
S_j	Saturation: volume of fluid per unit of porous volume.	
$y_{i,j}$	Molar fraction	
u_j	Darcy Velocity	m • min^{-1}
$\hat{q}_i$	Molar flux - source/sink	mol • m^{-3} • min^{-1}
q_i	Molar source/sink	mol • min^{-1}
A	Area	m^2
V_B	Block volume	m^3
k_{rj}	Relative permeability	
μ_j	Viscosity	Pa • min
k	Permeability	m^2
P	Pressure	Pa
D	Depth	m
U_j	Internal energy	J • mol^{-1}
T	Temperature	K
$q_{h,i}$	Thermal sink and sources	J • min^{-1}
α	Thermal conductivity	J • m^{-1} • min^{-1} • K^{-1}
$\dot{Q}_{conv}$	Heat transfer by convection	J • min^{-1}
$\dot{Q}_{cond}$	Heat transfer by conduction	J • min^{-1}
ΔH^r_{reac}	Reaction enthalpy	J • mol^{-1}
Cp_i	Heat capacity	J • mol^{-1} • K^{-1}
h_j	Enthalpy	J • mol^{-1}
$\hat{c}_R$	Average rock compressibility	Pa^{-1}
$\hat{c}_f$	Average fluid compressibility	Pa^{-1}
$\hat{c}_T$	Average thermal expansion coefficient	K^{-1}
V_P	Porous volume	m^3
Ω	Control volume	m^3
X, Y, Z	Cartesian coordinates	m
INDEX-i	Species oil, water, CO, CO_2, N_2, O_2	
INDEX-j	Phases oil, water, gas and solid	
INDEX-k	Position index for Z coordinate	
INDEX-r	Reaction index	
INDEX-nc	Number of species	
INDEX-np	Number of phases	
INDEX-nr	Number of reactions	
SATP	Standard Ambient Temperature and Pressure.	25°C /1atm

APPENDIX A

Table A1. Physical properties for solid, liquid and gas components.

Specie	Heat capacity as function of temperature $\left[\frac{j}{mol \cdot K}\right]$ $C_p = a + bT + cT^2 + dT^3$				Molecular weight $\left[\frac{kg}{kmol}\right]$	Mass density $\left[\frac{kg}{m^3}\right]$	Thermal conductivity $\left[\frac{j}{m \cdot min \cdot K}\right]$
	a	b	c	d			
$Coke_1$	17.00	-	-	-	673.04	1380	312.50
$Coke_2$	17.00	-	-	-	179.76	1380	312.50
Oil	1138.80	-	-	-	537.60	1008	7.98
Water	32.24	1.924×10^{-3}	1.055×10^{-5}	3.596×10^{-9}	18.02	1000	37.15
N_2	31.15	-1.357×10^{-2}	2.680×10^{-5}	-1.168×10^{-8}	28.02	Ideal Gas	1.25
O_2	28.11	-3.680×10^{-6}	1.746×10^{-5}	-1.065×10^{-8}	32.00	Ideal Gas	1.25
CO	30.87	-1.285×10^{-2}	2.789×10^{-5}	-1.272×10^{-8}	28.01	Ideal Gas	1.25
CO_2	19.80	7.344×10^{-2}	5.602×10^{-5}	1.715×10^{-8}	44.01	Ideal Gas	1.25
Rock matrix[1]	1.21×10^6	-	-	-	-	-	258.33

*Rock matrix heat capacity is calculated using rock volume. Units are presented as $\left[\frac{J}{m^3 \cdot K}\right]$

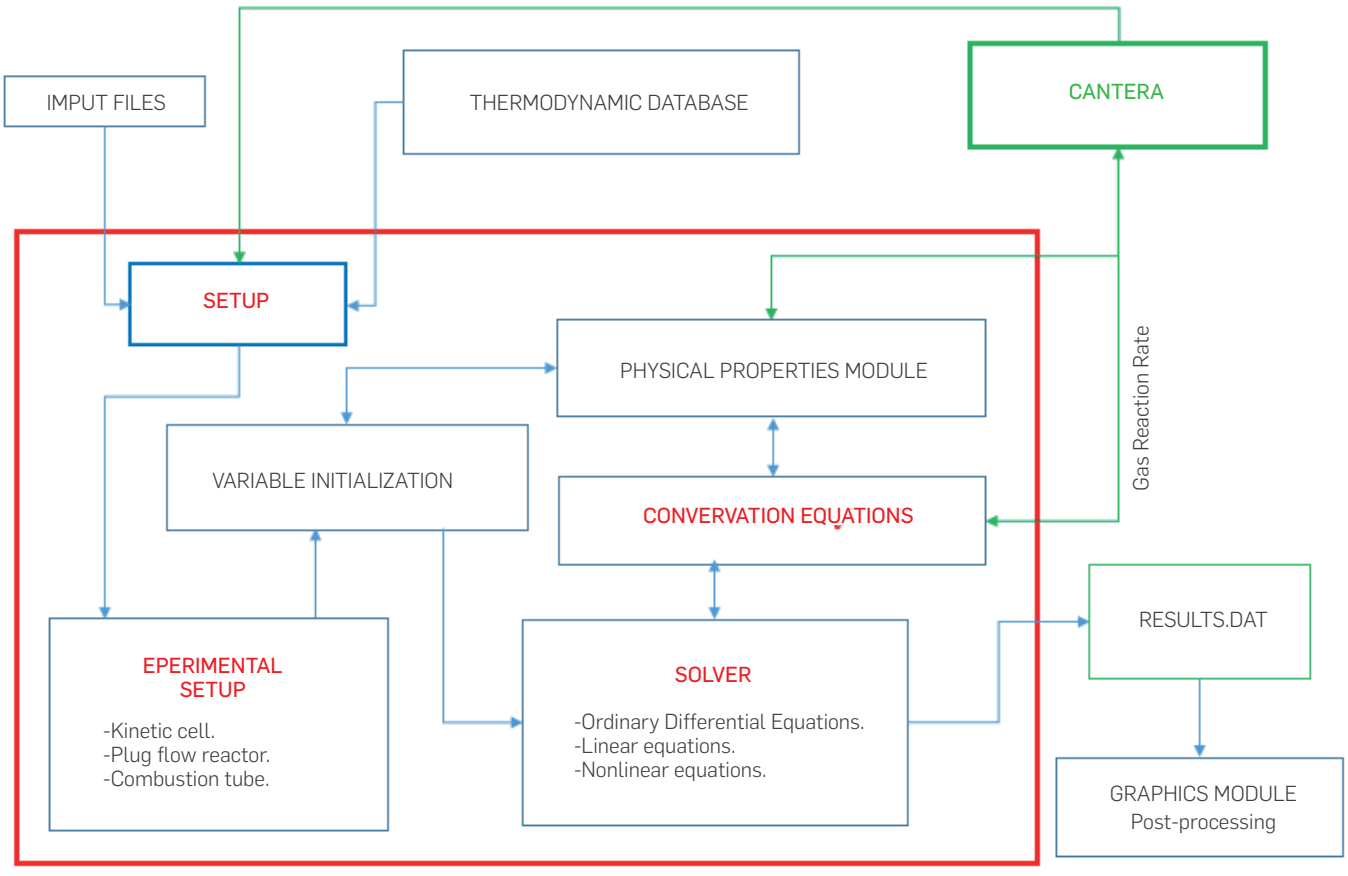

Figure A1. Schematic structure of the Toolbox.